SOFIA FIFI-LS Observations of [OIII] and [NIII] Lines to Measure Metallicity in Galaxies

Luigi Spinoglio, IAPS-INAF, Rome, Italy - SOFIA Tele-Talk 9 February 2022

My collaborators:

Juan Antonio Fernandez-Ontiveros (IAPS-INAF + CEFCA), Matt Malkan & Suyash Kumar (UCLA, Los Angeles),

Miguel Pereira-Santaella (CAB-INTA, Madrid), Enrique Perez-Montero & Borja Perez-Diaz (IAA-CSIC, Granada)

We measured the [OIII] and [NIII] far-IR fine structure lines in a sample of local galaxies, (Starburst/HII region galaxies, Seyfert and Dwarf galaxies) SOFIA FIFI-LS spectra of 25 objects plus other 31 galaxies observed with Herschel-PACS.

We found that the IR measure of N/O is significantly lower than its optical measure. We explored, as possible reasons of such a discrepancy, the different regimes traced by IR and optical lines in terms of ionization, density and extinction, however no significant correlation has been found. We suggest that the origin of this discrepancy might be due to the metallicity evolution of the different stellar populations after the accretion of metal-poor gas.

motivations

- explore the behavior of the N/O ratio:
- in young stellar populations it is dominated by primary O and N production.
- When the population evolves, the N abundance is increased by the secondary production due to the yield of intermediate mass stars.
- While O/H provides information on the total amount of heavy elements produced, the N/O ratio tells us how these elements have been formed.

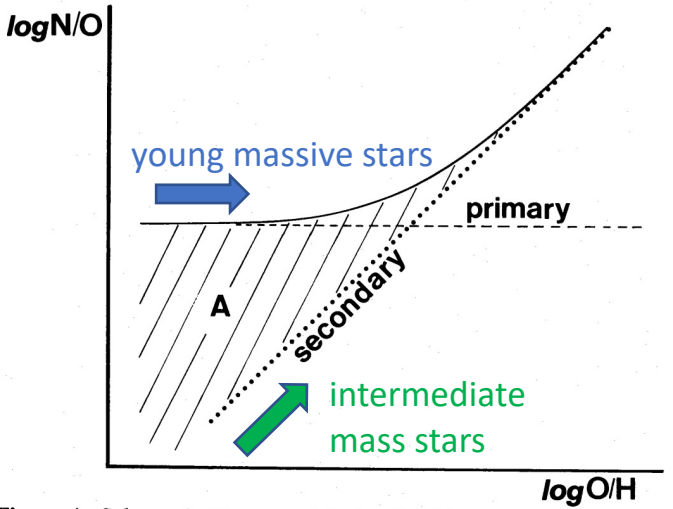

Figure 4. Schematic diagram of the log(N/O) versus log(O/H) plot if nitrogen has both a primary and a secondary component. The

Vila-Costas & Edmund 1993

- measuring abundances through IR fine-structure lines has major advantages wrt optical lines, as the former do not suffer extinction, have a negligible dependence on gas temperature and a weak dependence on gas density.
- with the ALMA observatory FIR lines can be observed in galaxies at high redshift and thus abundances measured ([Niii]57μm @ z> 7, ([Oiii]88μm @ z> 3, ([Nii]122μm @ z> 2)

IR fine-structure lines have negligible dependence on gas temperature

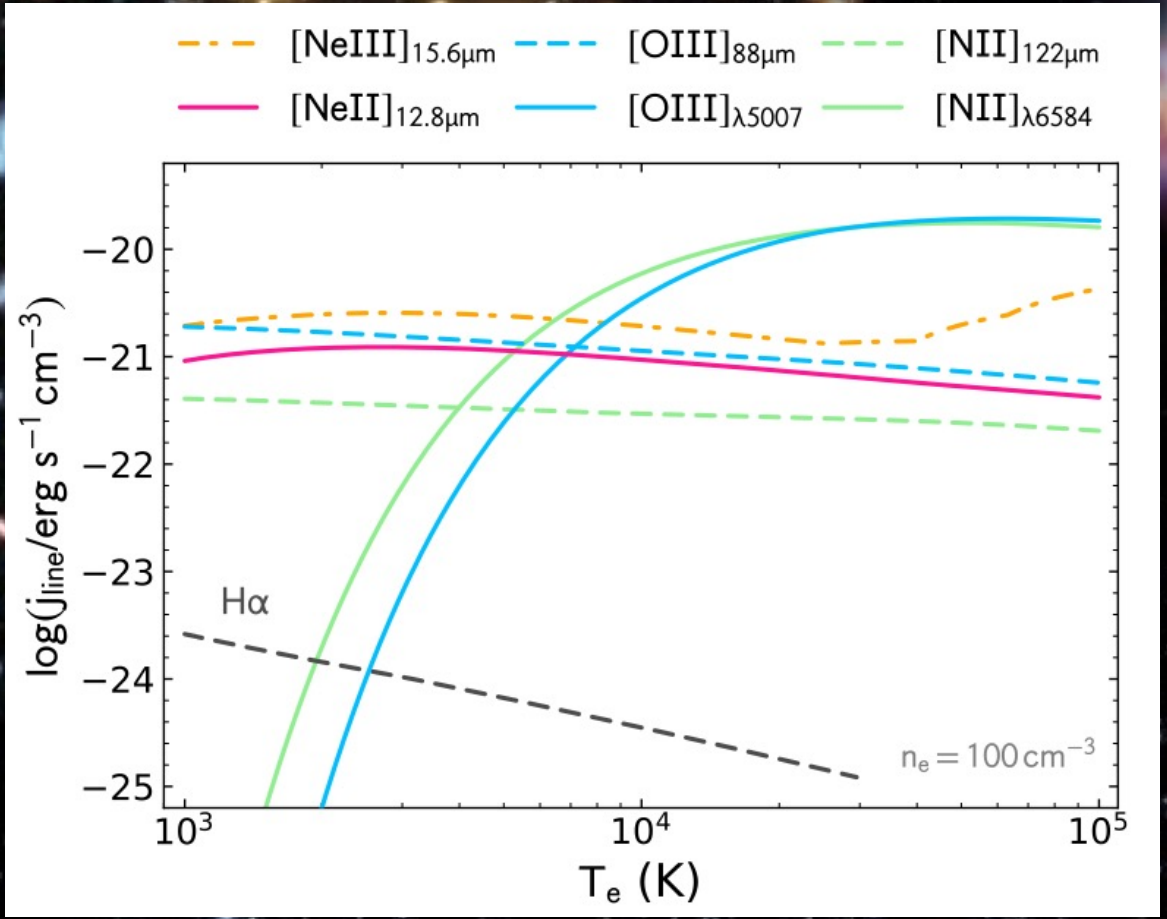

The emissivity ($j$line) of the fine-structure lines in the optical range (blue solid line: [Oiii] λ5007; green solid: [Nii] λ6584) is a strong function of the electron temperature T_e in the 2000–30000K range, in contrast with the IR lines (pink solid: [Ne ii]12.8 μm; orange dot-dashed: [Neiii]15.6μm; blue dashed: [Oiii]88μm; green dashed: [N ii]122 μm). [Fernandez-Ontiveros et al 2021]

Observational framework of optical data to measure N/O vs. O/H and their interpretation

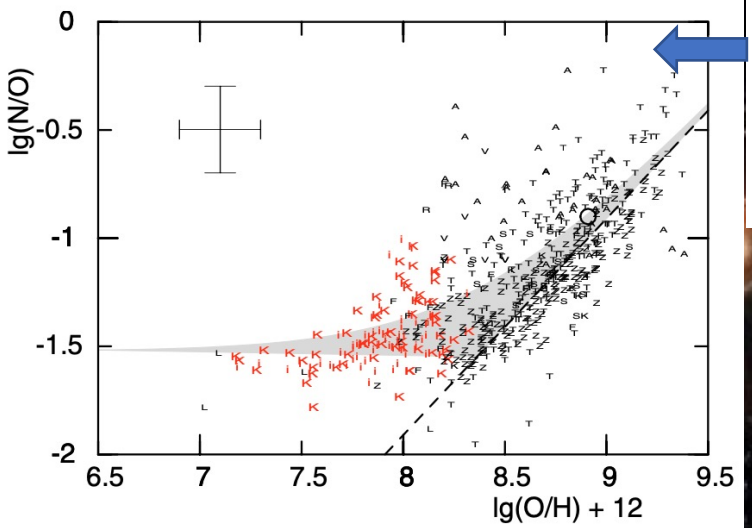

N/O as a function of oxygen abundance observed in spiral galaxies and irregular galaxies after Henry & Worthey (1999)

SDSS data sample for the (N/O) versus (O/H) compared with star-forming dwarf galaxies.

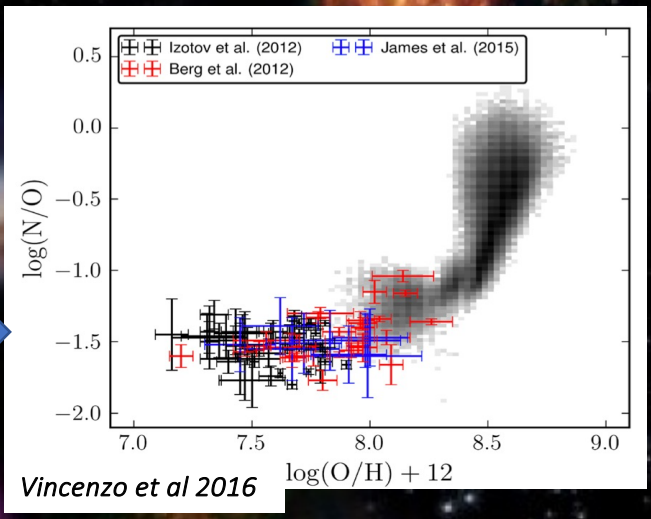

Vincenzo et al 2016

Green Peas show larger N/O than HII regions of similar O/H.
this is a possible signpost of recent massive accretion of metal poor gas.

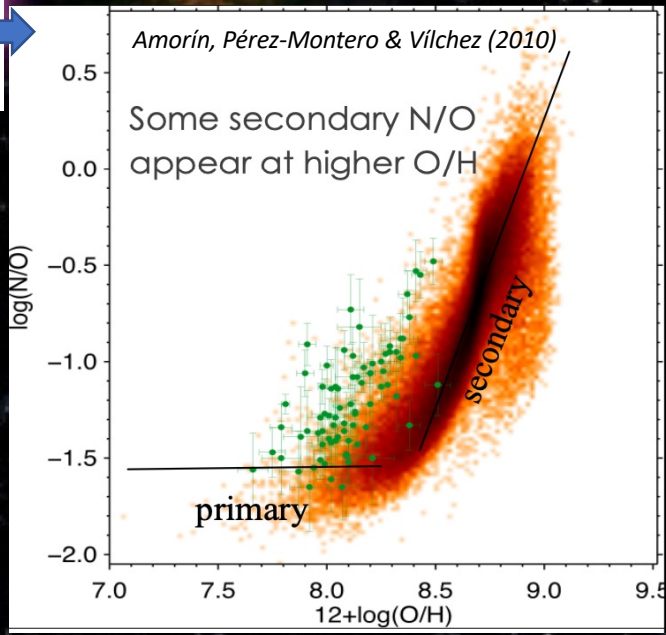

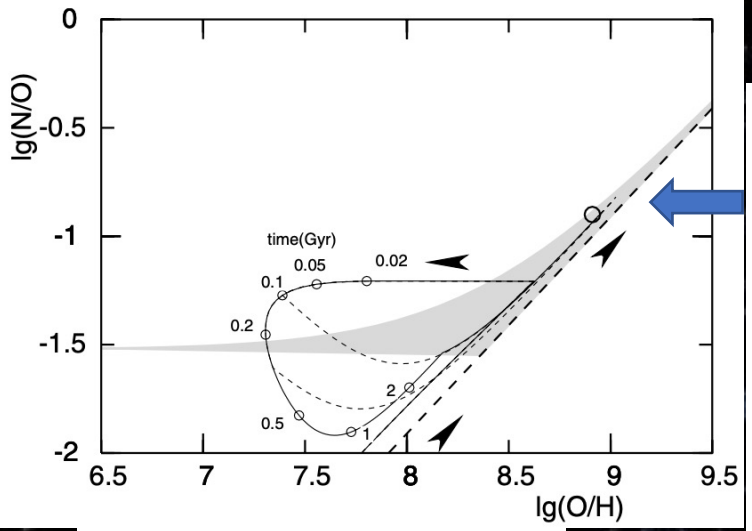

Köppen & Hensler 2005

Effect of gas infall:
Time evolution of models with an infall rate of 100 galaxy masses per Gyr, starting at an age of 5 Gyr.

The N/O ratio depends on the accretion of pristine external gas, on the shape of the IMF, the SF efficiency and the efficiency of galactic winds in removing metals from the ISM.

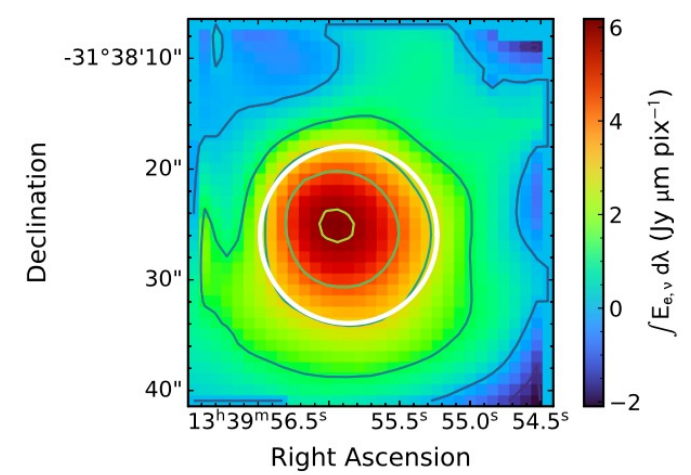

(a)

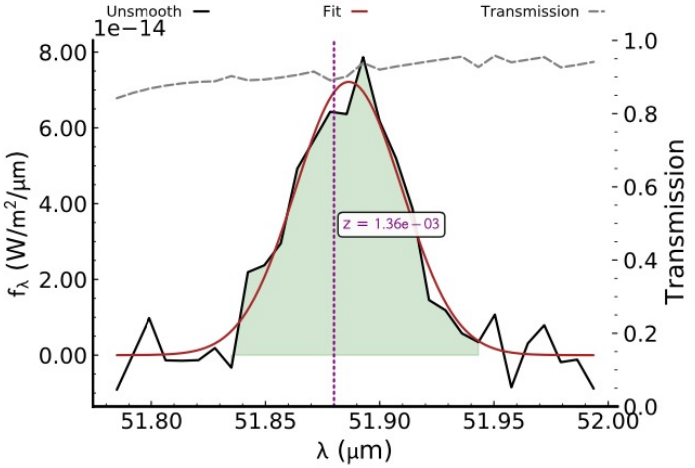

(b)

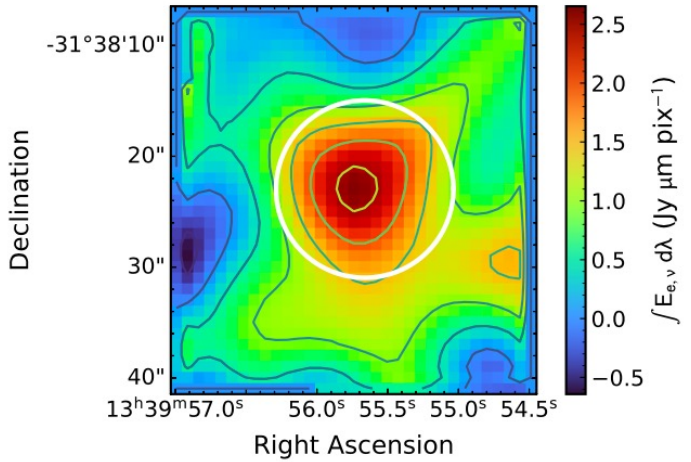

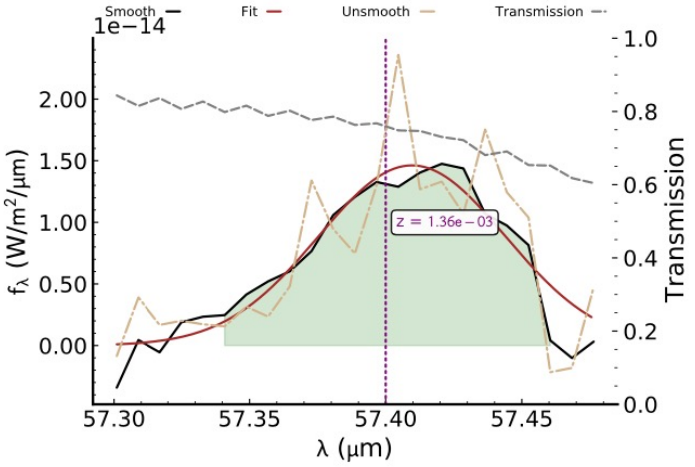

(d)

Spinoglio et al. (2021), ApJ, in press & astro-ph: 2103.09253

example of the SOFIA FIFI-LS data reduction: NGC5253: top: [Oiii]52 bottom: [Niii]57μm.

Abundance determinations

- Two independent abundance determinations ➔O/H and N/O ratios using:
  (1) optical nebular lines [the Hii-Chi-mistry (Perez-Montero+2019)]and
  (2) IR nebular lines [Hii-Chi-mistry-IR codes (Fernandez-Ontiveros+2021)]
- Both based on the same grid of photo-ionization models (Cloudy; Ferland+2017):
  - HII region/(U)LIRG: stellar population models from Popstar (Molla+2009) with a constant electron density of n_e= 100 cm^{-3},
  - AGN: a power-law ionizing continuum
    ($F_\nu \propto \nu^{-0.8}$) and n_e= 500 cm^{-3} (Perez-Montero2019}.

Journal of SOFIA observations reduced

total sample discussed: 47 galaxies

optical O/H & N/O

IR O/H & N/O

Table 1. Journal of the SOFIA FIFI-LS observations

Target	RA	dec	z	Type	AOR-ID	Mission-ID	PI	line	T_{exp} (s)
(1)	(2)	(3)	(4)	(5)	(6)	(7)	(8)	(9)	(10)
MCG+12-02-001	00h 54m 03.6s	+73d 05m 12s	0.015698	ULIRG	07_0209_11	2019-05-01_FI_F562	G. Stacey	[OIII]$_{52\mu m}$	1320.96
MCG+12-02-001	" "	" "	"	"	07_0209_12	2019-05-01_FI_F562	G. Stacey	[NIII]$_{57\mu m}$	1351.68
NGC1365	03h 33m 36.4s	-36d 08m 26s	0.005457	S1.8	05_0111_3	2017-07-28_FI_F424	G. Stacey	[OIII]$_{52\mu m}$	1843.20
IC342	03h 46m 48.5s	+68d 05m 47s	0.000103	HII	03_0135_9	2015-03-26_FI_F205	K. Croxall	[OIII]$_{52\mu m}$	967.68
NGC1569	04h 30m 49.0s	+64d 50m 53s	-0.000347	Dwarf	87_0005_7	2014-04-22_FI_FO162	R. Klein	[OIII]$_{52\mu m}$	14976.50
NGC1569	" "	" "	"	"	07_0048_2	2019-05-02_FI_F563	J. Spilker	[NIII]$_{57\mu m}$	2805.76
NGC1614	04h 34m 00.0s	-08d 34m 45s	0.015938	HII	07_0209_14	2019-10-30_FI_F631	G. Stacey	[OIII]$_{52\mu m}$	522.24
NGC1614	" "	" "	"	"	07_0209_15	2019-10-30_FI_F631	G. Stacey	[NIII]$_{57\mu m}$	1136.64
NGC1808	05h 07m 42.3s	-37d 30m 46s	0.003319	HII	05_0111_3	2017-07-28_FI_F424	G. Stacey	[OIII]$_{52\mu m}$	1751.04
IIZw40	05h 55m 42.7s	+03d 23m 32s	0.002632	Dwarf	06_0225_5	2018-11-06_FI_F524	G. Stacey	[OIII]$_{52\mu m}$	768.00
IIZw40	" "	" "	"	"	06_0225_10	2018-11-06_FI_F524	G. Stacey	[NIII]$_{57\mu m}$	1536.00
NGC2146	06h 18m 37.8s	+78d 21m 25s	0.002979	HII	03_0135_2	2015-03-12_FI_F199	K. Croxall	[OIII]$_{52\mu m}$	368.69
NGC2146	" "	" "	"	"	03_0135_17	2015-03-12_FI_F199	K. Croxall	[NIII]$_{57\mu m}$	307.228
NGC2366	07h 28m 55.5s	+69d 13m 05s	0.000267	Dwarf	07_0239_6	2019-05-14_FI_F570	M.A. Malkan	[OIII]$_{52\mu m}$	614.40
NGC2366	" "	" "	"	"	07_0239_7	2019-05-14_FI_F570	M.A. Malkan	[NIII]$_{57\mu m}$	614.40
He2-10	08h 36m 15.2s	-26d 24m 34s	0.002912	Dwarf	70_0508_6	2017-02-25_FI_F378	A. Krabbe	[OIII]$_{52\mu m}$	1658.88
UGC5189	09h 42m 54.7s	+09d 29m 01s	0.01072	HII	07_0182_1	2019-05-09_FI_F568	T. Jones	[OIII]$_{52\mu m}$	2211.84
M82	09h 55m 52.2s	+69d 40m 48s	0.000677	HII	70_0408_1	2016-02-25_FI_F280	A. Krabbe	[OIII]$_{52\mu m}$	2918.40
M82	" "	" "	"	"	70_0608_10	2018-11-08_FI_F526	A. Krabbe	[NIII]$_{57\mu m}$	4177.92
Haro3	10h 45m 22.4s	+55d 57m 38s	0.003149	Dwarf	06_0225_6	2018-11-07_FI_F525	G. Stacey	[OIII]$_{52\mu m}$	1413.12
Mrk1271	10h 56m 09.1s	+06d 10m 22s	0.00338	HII	07_0182_3	2019-05-04_FI_F565	T. Jones	[OIII]$_{52\mu m}$	1720.32
Arp299A	11h 28m 30.4s	+58d 34m 10s	0.0103	HII	05_0111_5	2017-02-28_FI_F379	G. Stacey	[OIII]$_{52\mu m}$	2949.12
Arp299B&C	" "	" "	"	"	05_0111_5	2017-02-28_FI_F379	G. Stacey	[OIII]$_{52\mu m}$	2949.12
Pox4	11h 51m 11.6s	-20d 36m 02s	0.01197	HII	07_0182_2	2019-05-03_FI_F564	T. Jones	[OIII]$_{52\mu m}$	1259.52
Mrk193	11h 55m 28.3s	+57d 39m 52s	0.017202	HII	07_0182_4	2019-05-14_FI_F570	T. Jones	[OIII]$_{52\mu m}$	3164.16
NGC4194	12h 14m 09.5s	+54d 31m 37s	0.008342	HII	07_0209_16	2019-05-09_FI_F568	G. Stacey	[OIII]$_{52\mu m}$	430.08
NGC4194	" "	" "	"	"	07_0209_18	2019-05-09_FI_F568	G. Stacey	[NIII]$_{57\mu m}$	860.16
NGC4214	12h 15m 39.3s	+36d 19m 37s	0.00097	Dwarf	06_0225_8	2019-02-28_FI_F549	G. Stacey	[OIII]$_{52\mu m}$	1320.96
NGC4214	" "	" "	"	"	06_0225_9	2019-05-08_FI_F567	G. Stacey	[NIII]$_{57\mu m}$	1413.12
NGC4536	12h 34m 27.1s	+02d 11m 17s	0.006031	HII	03_0135_6	2015-03-27_FI_F206	K. Croxall	[OIII]$_{52\mu m}$	399.36
NGC4631	12h 42m 07.8s	+32d 32m 35s	0.002021	HII	07_0239_3	2019-05-10_FI_F569	M.A. Malkan	[OIII]$_{52\mu m}$	215.04
NGC4631	" "	" "	"	"	07_0239_3	2019-05-10_FI_F569	M.A. Malkan	[NIII]$_{57\mu m}$	1720.32
NGC4670	12h 45m 17.1s	+27d 07m 31s	0.003566	Dwarf	06_0222_21	2019-03-02_FI_F551	T. Wiklind	[OIII]$_{52\mu m}$	491.52
M83	13h 37m 00.9s	-29d 51m 56s	0.001711	HII	07_0209_8	2019-05-04_FI_F565	G. Stacey	[OIII]$_{52\mu m}$	2119.68
NGC5253	13h 39m 56.0s	-31d 38m 24s	0.001358	Dwarf	07_0239_4	2019-05-10_FI_F569	M.A. Malkan	[OIII]$_{52\mu m}$	307.20
NGC5253	" "	" "	"	"	07_0239_5	2019-05-10_FI_F569	M.A. Malkan	[NIII]$_{57\mu m}$	829.44

Name	RA	dec	z	Type	12+log(O/H)	log(N/O)	Refs.	12+log(O/H)$_{IR}$	log(N/O)$_{IR}$
(1)	(2)	(3)	(4)	(5)	(6)	(7)	(8)	(9)	(10)
Haro11	00h 36m 52.5s	-33d 33m 17s	0.020598	Dwarf	8.23±0.03	-0.92	M13,C19	8.51±0.07	-1.2±0.2
NGC253	00h 47m 33.1s	-25d 17m 19s	0.000811	HII	8.61±0.01	-0.43±0.04	TW	8.7±0.2	-0.4±0.2
MCG+12-02-001	00h 54m 03.6s	+73d 05m 12s	0.015698	LIRG	8.7	...	AH10	8.7±0.1	-1.0±0.1
NGC1068	02h 42m 40.7s	-00d 00m 48s	0.003793	S1h	8.60±0.06	-0.02±0.02	TW	...	-0.35±0.05
NGC1365	03h 33m 36.4s	-36d 08m 26s	0.005457	S1	8.88±0.02	...	TW	...	-0.3±0.05
NGC1569	04h 30m 49.0s	+64d 50m 53s	-0.000347	Dwarf	8.19±0.03	-1.39	M13,C19	7.7±0.2	-1.6±0.1
NGC1614	04h 34m 00.0s	-08d 34m 45s	0.015938	HII	8.60±0.01	-0.56±0.03	TW	8.69±0.08	-1.0±0.1
NGC1808	05h 07m 42.3s	-37d 30m 46s	0.003319	HII	8.71±0.01	-0.4±0.1	TW	8.5±0.3	-0.8±0.3
IIZw40	05h 55m 42.6s	+03d 23m 32s	0.002632	Dwarf	8.09±0.02	-1.44	M13,C19	7.7±0.2	...
Mrk3	06h 15m 36.4s	+71d 02m 15s	0.013509	S1h	8.69±0.07	-0.55±0.03	TW	...	-0.9±0.1
NGC2146	06h 18m 37.8s	+78d 21m 25s	0.002979	LIRG	8.71±0.02	-0.77±0.03	TW	8.7±0.1	-0.9±0.1
NGC2366	07h 28m 55.6s	+69d 13m 05s	0.000267	Dwarf	7.64±0.03	...	M13		...
He2-10	08h 36m 15.2s	-26d 24m 34s	0.002912	Dwarf	8.65±0.01	-0.75±0.01	TW	8.64±0.08	-1.0±0.1
IRAS08572+3915	09h 00m 25.4s	+39d 03m 54s	0.05835	ULIRG	8.62±0.02	-0.96±0.05	TW	8.5±0.2	-0.7±0.2
UGC5101	09h 35m 51.6s	+61d 21m 11s	0.01615	ULIRG	8.78±0.02	-0.7±0.1	TW	8.6±0.1	-0.6±0.4
M82	09h 55m 52.7s	+69d 40m 46s	0.00068	HII	8.70±0.01	-0.46±0.03	TW	8.6±0.1	-0.8±0.2
NGC3256	10h 27m 51.3s	-43d 54m 13s	0.00935	HII	8.39±0.07	-0.39±0.02	TW	8.70±0.09	-0.80±0.09
Haro3	10h 45m 22.4s	+55d 57m 38s	0.003149	Dwarf	8.37±0.02	-1.35	M13,C19	8.30±0.07	-1.4±0.1
IRAS10565+2448	10h 59m 18.2s	+24d 32m 34s	0.04310	ULIRG	8.77±0.02	-0.50±0.01	TW	8.6±0.1	-0.6±0.1
IRAS11095-0238	11h 12m 03.4s	-02d 54m 23s	0.106634	ULIRG	8.53±0.02	-0.77±0.09	TW	8.7±0.1	-0.9±0.3
Arp299 A=IC694	11h 28m 33.7s	58d 33m 49s	0.01041	LIRG	8.56±0.02	-0.74±0.02	TW	8.5±0.1	-1.0±0.1
Arp299 B+C=NGC3690	11h 28m 31.0s	58d 33m 43s	0.01022	LIRG	8.79±0.02	-0.50±0.01	TW	8.6±0.1	-1.0±0.1
NGC4151	12h 10m 32.6s	+39d 24m 21s	0.003319	S1	8.5±0.1	-0.71±0.07	TW	...	-0.59±0.06
IRAS12112+0305	12h 13m 46.0s	+02d 48m 38s	0.073317	ULIRG	8.66±0.02	-0.75±0.01	TW	8.4±0.2	-0.5±0.2
NGC4194	12h 14m 09.5s	+54d 31m 37s	0.008342	LIRG	8.52±0.01	-0.63±0.03	TW	8.5±0.2	-0.9±0.1
NGC4214-reg.1	12h 15m 39.3s	+36d 19m 37s	0.00097	Dwarf	8.20±0.03	...	M13	8.6±0.1	-1.4±0.1
NGC4631	12h 42m 07.8s	+32d 32m 35s	0.002021	HII	8.52±0.01	-1.11±0.03	TW	8.69±0.07	...
NGC4945	13h 05m 27.5s	-49d 28m 06s	0.00188	S2	...	...		8.5±0.4	-0.6±0.2
NGC5033	13h 13m 27.5s	+36d 35m 38s	0.00292	S2	8.85±0.07	-0.25±0.01	TW	...	-0.73±0.07
IRAS13120-5453	13h 15m 06.4s	-55d 09m 23s	0.03076	ULIRG	...	...		8.7±0.1	-0.7±0.2
CenA=NGC5128	13h 25m 27.6s	-43d 01m 09s	0.00183	S2	8.85±0.02	-0.91±0.04	TW	...	-0.92±0.08
M83	13h 37m 00.9s	-29d 51m 56s	0.001711	HII	8.6±0.2	-0.34±0.02	TW	8.7±0.1	-0.7±0.2
NGC5253	13h 39m 56.0s	-31d 38m 24s	0.001358	Dwarf	8.16±0.03	-1.45	M13,C19	8.2±0.1	-1.2±0.1
Mrk273	13h 44m 42.1s	+55d 53m 13s	0.03778	S2	8.85±0.06	-1.06±0.07	TW	...	-0.8±0.2
IC4329A	13h 49m 19.3s	-30d 18m 34s	0.016054	S1	8.4±0.2	-1.0±0.4	TW	...	-0.77±0.07
Mrk463E	13h 56m 02.9s	+18d 22m 18s	0.05035	S1h	8.5±0.2	-1.0±0.4	TW	...	-0.9±0.1
Circinus	14h 13m 09.9s	-65d 20m 21s	0.00145	S1h	8.8±0.1	-0.4±0.1	TW	...	-0.74±0.02
NGC5506	14h 13m 14.9s	-03d 12m 28s	0.006181	S1h	8.76±0.07	-1.1±0.3	TW	...	-0.81±0.05
NGC6240	16h 52m 58.9s	+02d 24m 04s	0.02448	LIN	8.85±0.01	-1.1±0.1	TW	...	-0.9±0.2
IRAS17208-0014	17h 23m 21.9s	-00 d17m 01s	0.042810	ULIRG	8.69±0.01	-0.61±0.03	TW	8.7±0.1	-0.8±0.2
3C405=Cyg A	19h 59m 28.3s	+40d 44m 02s	0.056075	S2	8.78±0.04	-0.50±0.06	TW	...	-1.0±0.2
IRAS20551-4250	20h 58m 26.8s	-42d 39m 00s	0.042996	ULIRG	8.50±0.01	-0.83±0.05	TW	8.70±0.09	-0.9±0.2
NGC7130=IC5135	21h 48m 19.5s	-34d 57m 05s	0.01615	S2	8.60±0.09	-0.6±0.3	TW	...	-0.4±0.1
NGC7172	22h 02m 01.9s	-31d 52m 11s	0.00868	S2	8.8±0.2	...	TW	...	-0.7±0.1
NGC7314	22h 35m 46.2s	-26d 03m 02s	0.004763	S1h	8.88±0.02	-0.2±0.2	TW	...	-1.03±0.05
NGC7469	23h 03m 15.6s	+08d 52m 26s	0.01632	S1	8.4±0.1	-0.38±0.03	TW	...	-0.4±0.1
IRAS23128-5919	23h 15m 46.8s	-59d 03m 16s	0.04460	ULIRG	8.40±0.07	-0.75±0.01	TW	8.48±0.07	-0.8±0.1
NGC7582	23h 18m 23.7s	-42d 22m 14s	0.005254	S1h	8.5±0.1	-0.47±0.02	TW	...	-0.71±0.06

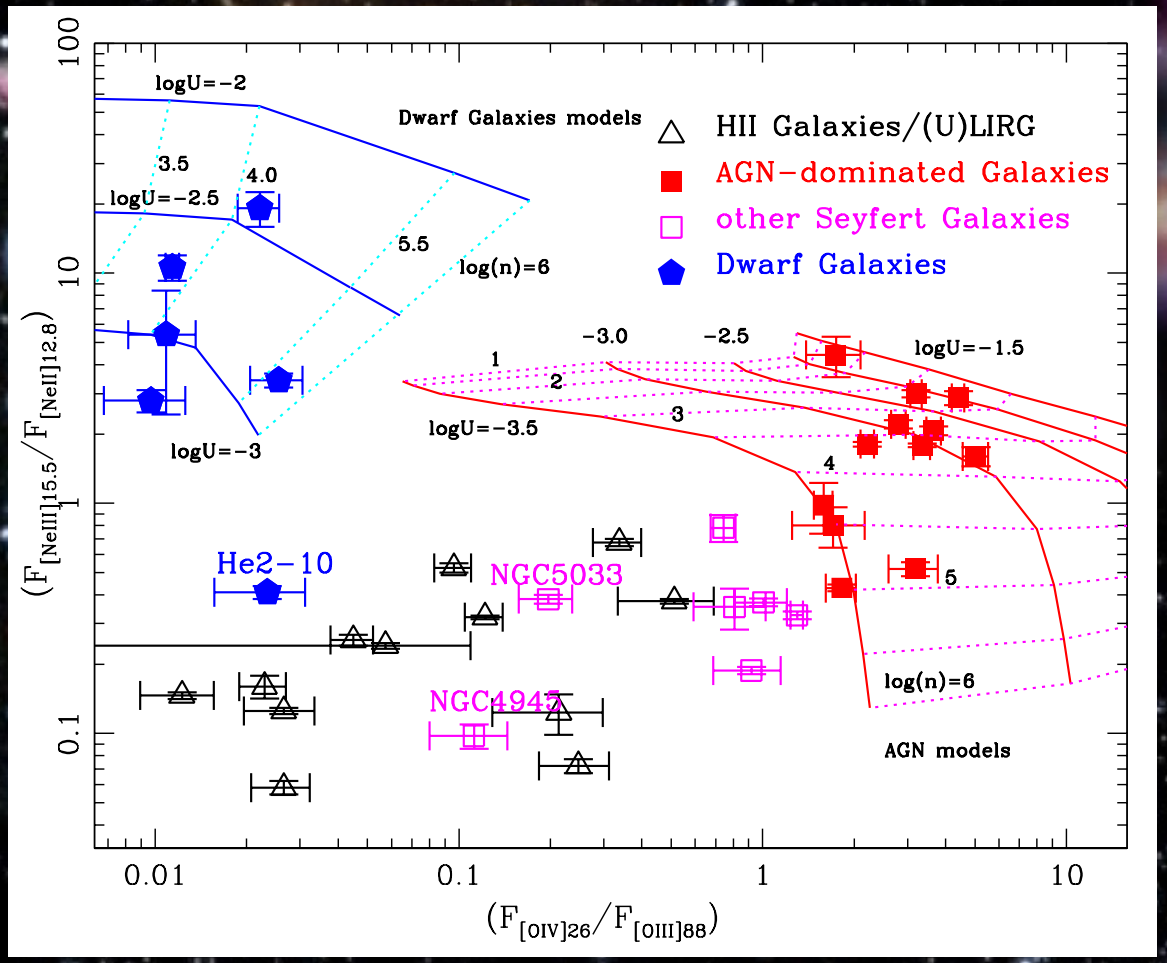

Spinoglio et al. (2021), ApJ, in press & astro-ph: 2103.09253

Our sample of local galaxies contains 47 galaxies divided in 21 HII region/(U)LIRG galaxies, 19 Seyfert galaxies, including one LINER and 7 dwarf galaxies.

We classified the sample of galaxies using the so called "IR BPT diagram", separating:

- AGN-dominated galaxies (red)
- other (lower excitation) Seyfert galaxies (magenta)
- HII region/(U)LIRG galaxies (black)
- Dwarf galaxies (blue)

[Fernandez-Ontiveros+2016, ApJ]

we tested the Σ[OIII]/[NIII] ratio as a f(metallicity)

[OIII]52µm, [OIII]88µm and [NIII]57µm were proposed by Nagao et al. (2011) and applied to Herschel observations by Pereira-Santaella et al. (2017) , Herrera-Camus et al. (2018). (2.2×[OIII]88µm + [OIII]52µm/[NIII]57µm) can trace the global N/O ratio. However, a previous knowledge of the O/H–N/O relation is needed, which depends on the star formation histories. This is shown by the data scatter in the vertical axis. As shown by the upper and lower dashed green model lines, the log(N/O) ratio ranges by a factor of at least +/-2.3X. A definite metallicity measure can be made only with a measured value of N/O.

ULIRGs + Dwarfs

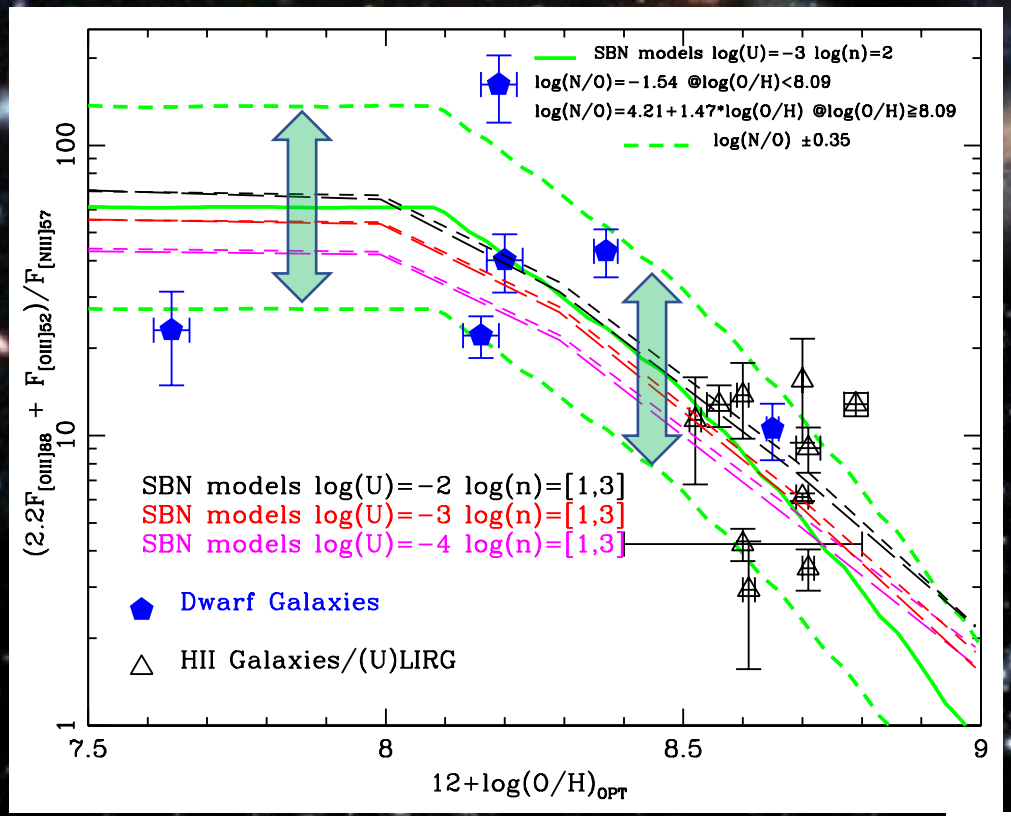

AGN-dominated + other Seyfert's

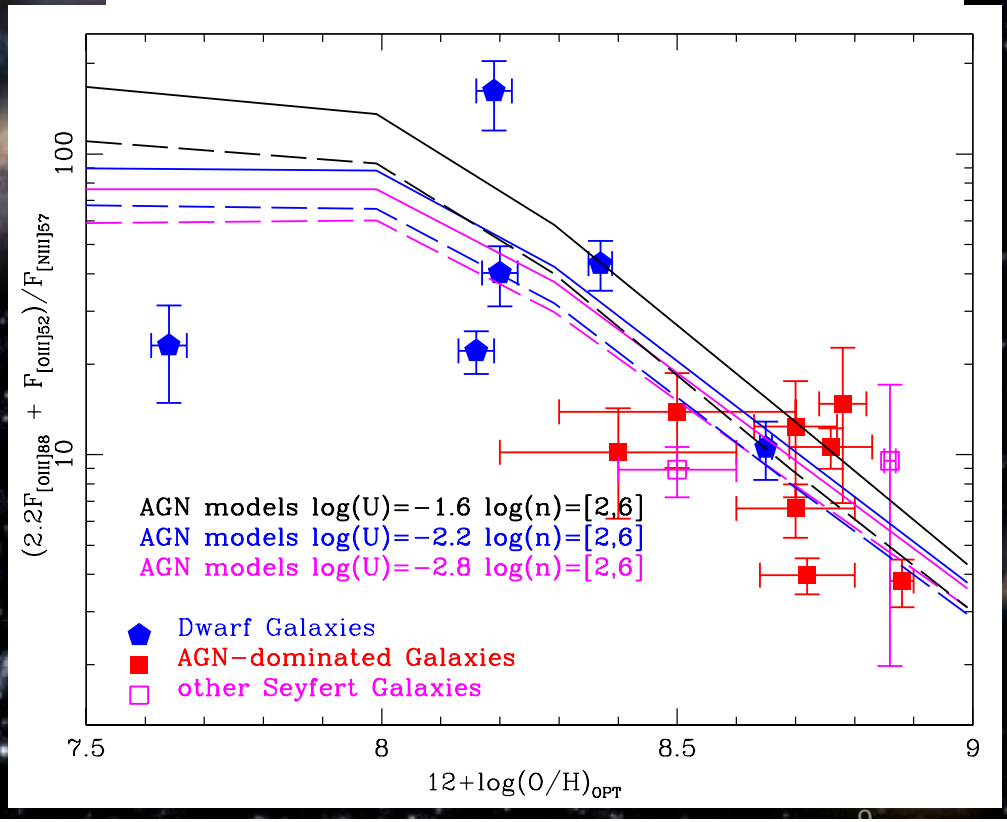

Spinoglio et al. (2021), ApJ, in press & astro-ph: 2103.09253

[Oiii]88/[Niii]57 vs O/H

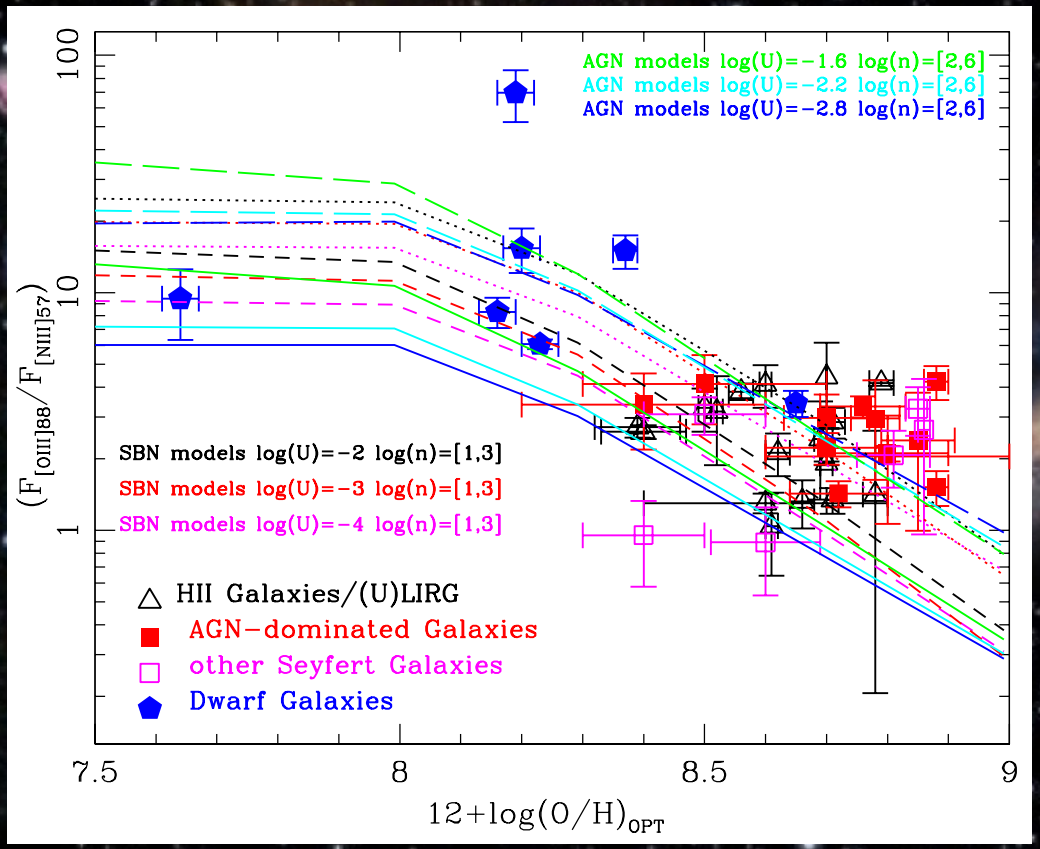

[Oiii]88/[Nii]122 vs O/H

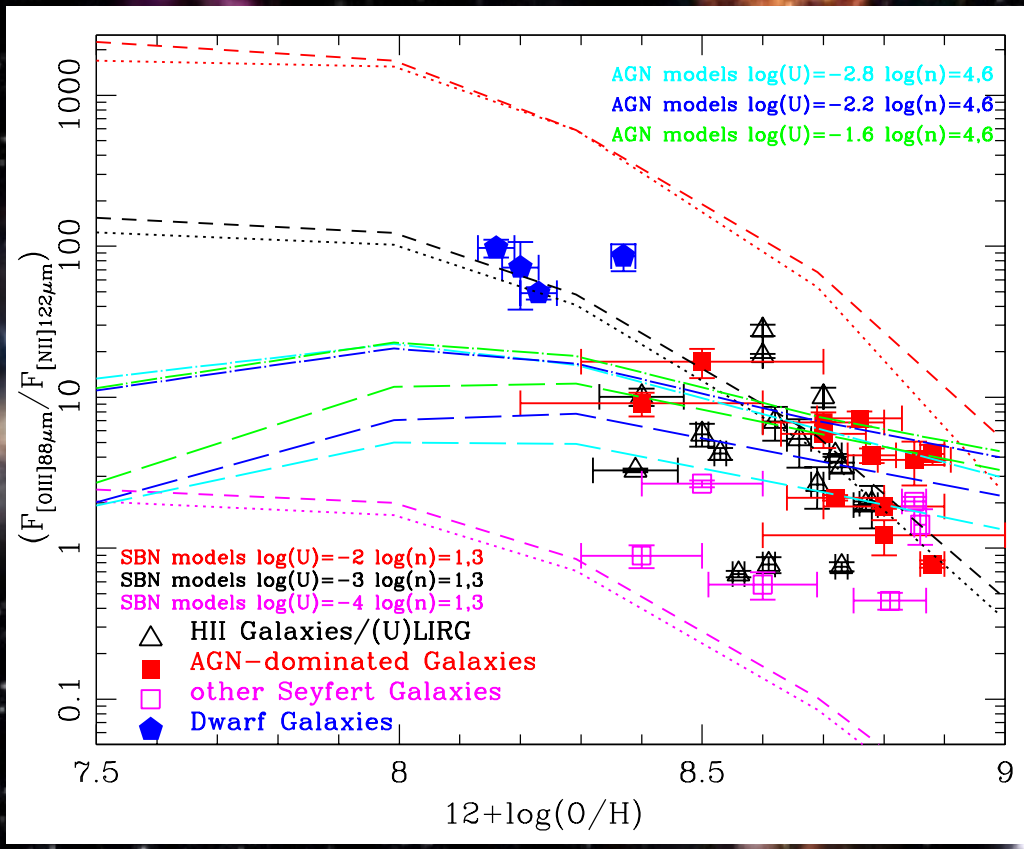

the other line ratios from FIR lines that can be used to measure abundances, [Oiii]88μm/[Niii]57μm and [Oiii]88μm/[Nii]122μm, have a larger dependence on both the density and the ionization potential (as shown by photoionization models)

(N/O)OPT vs (O/H)OPT: cluster around solar value (log(N/O)solar=-0.625). <log(N/O)OPT> = -0.73±0.34

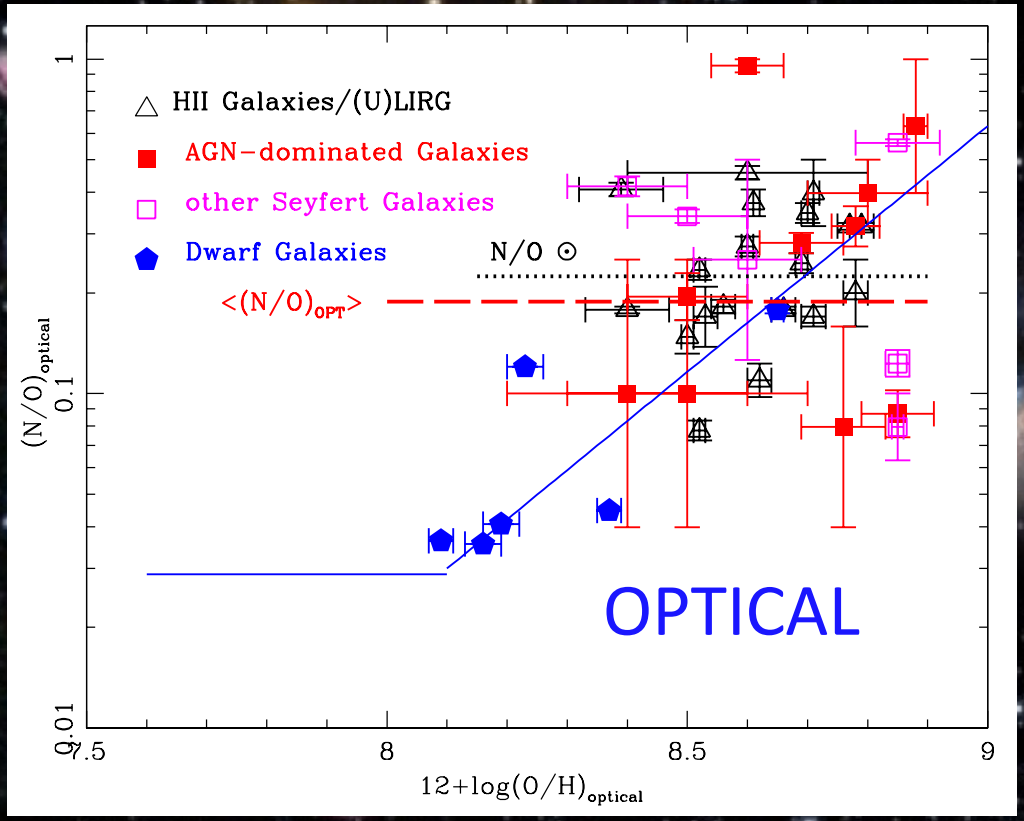

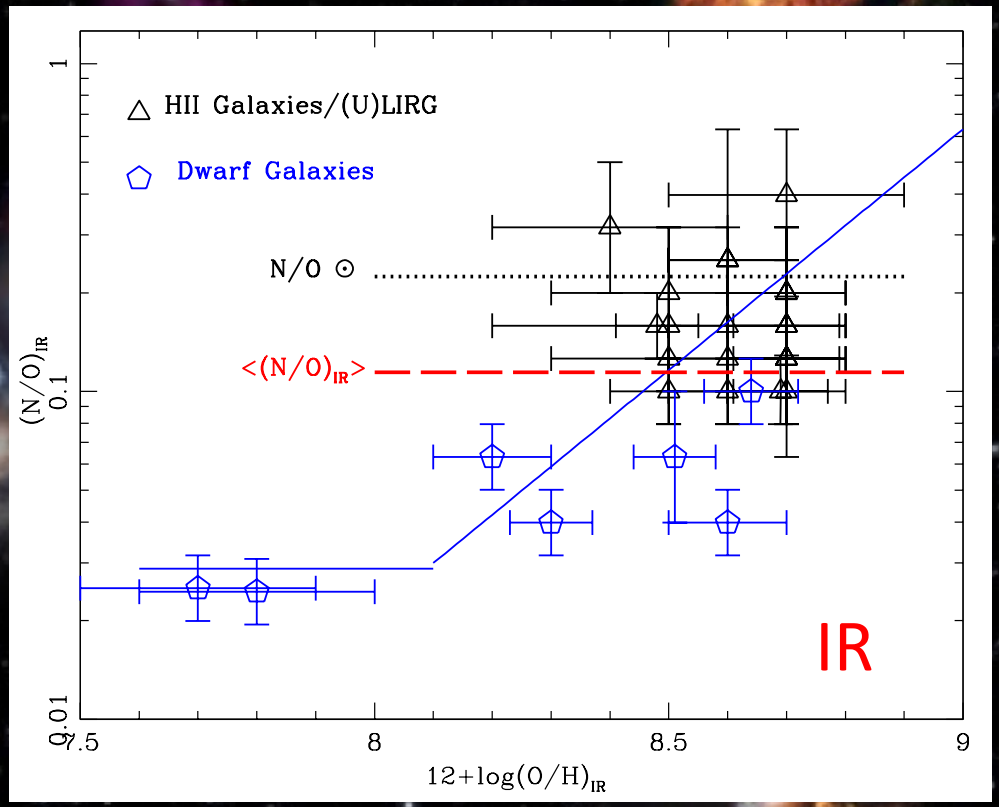

(N/O)IR vs (O/H)IR: far from solar value
<log(N/O)IR> = -0.94±0.30

The Pilyugin et al. (2014) relation between N and O is shown as a solid line, for comparison, which assumes:
log(N/O) = -1.54 for: [12+log(O/H)]< 8.1. and
log(N/O) = 4.21 + 1.47×[log(O/H)] for: [12+log(O/H)]> 8.1.

Spinoglio et al. (2021), ApJ, in press & astro-ph: 2103.09253

(O/H)IR vs (O/H)OPT: agree within the errors

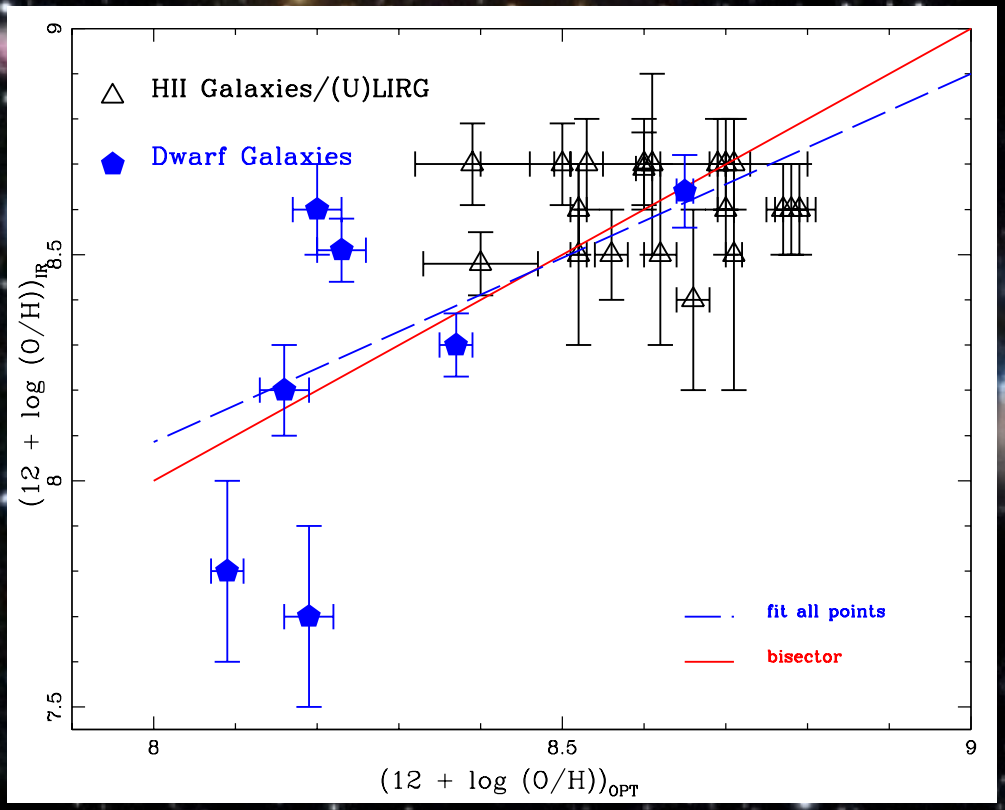

(N/O)IR vs (N/O)OPT: disagree at high (N/O)

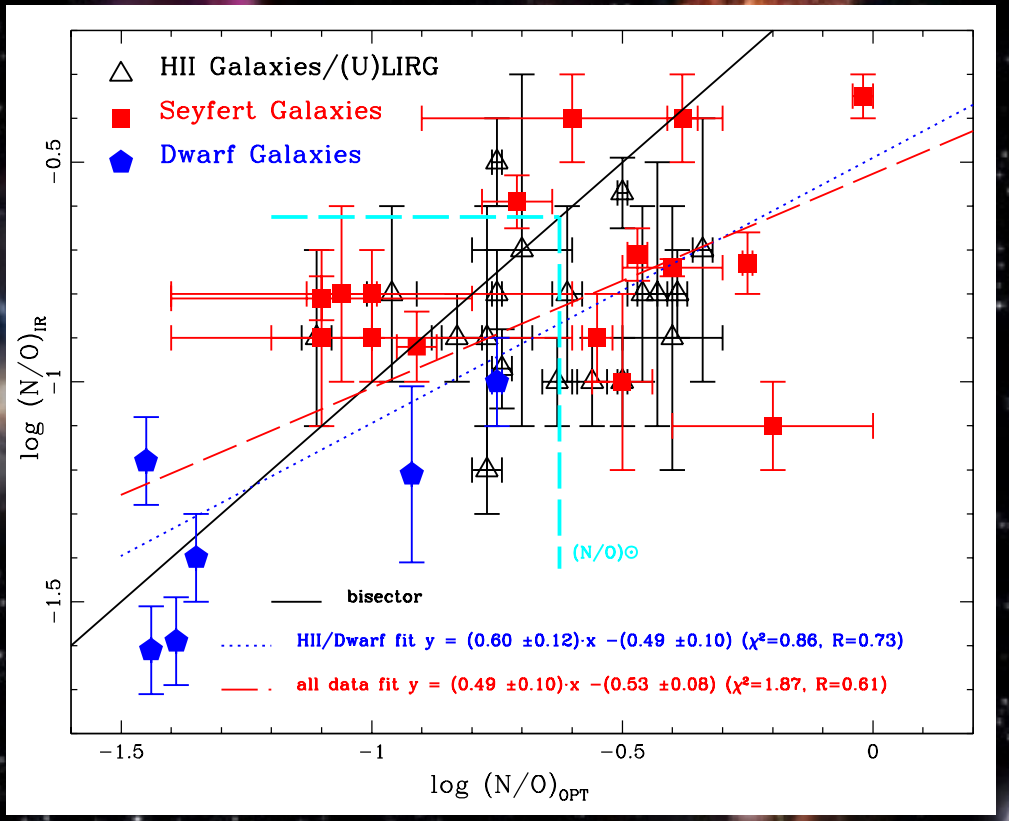

N/O ratio derived from IR, using the method from IR lines of Fernandez-Ontiveros et al. (2021) is compared to the N/O ratio computed from the optical lines using Perez-Montero (2014). This result shows a systematic difference between the two N/O determinations (Spinoglio et al. 2021).

Explore why the discrepancy in the N/O(OPT-IR)

Three main scenarios:

- difference in the ionization structure ➔ lower N/O ratios by IR:
  - IR tracers probe higher ionization gas (O++ and N++) closer to massive stars, where the primary production of N is prevalent,
  - optical lines trace lower ionization gas (O+ and N+) with a higher N enrichment from a secondary origin.
- contamination by DIG(Diffuse Ionized Gas) affecting the N lines in the optical range
  - Hot and low-density gas (DIG; e.g. Vale Asari et al. 2019) in the ISM (proposed by Peng et al. 2021) could account for ∼ 30% of the optical line fluxes of the [OII]λλ3727, 3729 and the [NII]λλ6548, 6584 doublets, while the effect of this contribution on the higher ionization transitions in the IR would be negligible.
- dust obscuration affects the optical-based determinations.
  - Optical lines were corrected by extinction (Balmer decrement), however they do not trace the obscured/embedded star-forming regions and AGN that IR lines probe.
  - Optical lines trace preferentially the enrichment with secondary N in the less obscured regions. Uncorrected obscuration affecting the [OII]λλ3727, 3729 doublet would particularly affect the optical N/O abundances, since the N lines are less affected by extinction.

Δ(N/O)≡(N/O)OPT-(N/O)IR search dependence of Δ(N/O) on ionization: [Neiii]/[Neii]

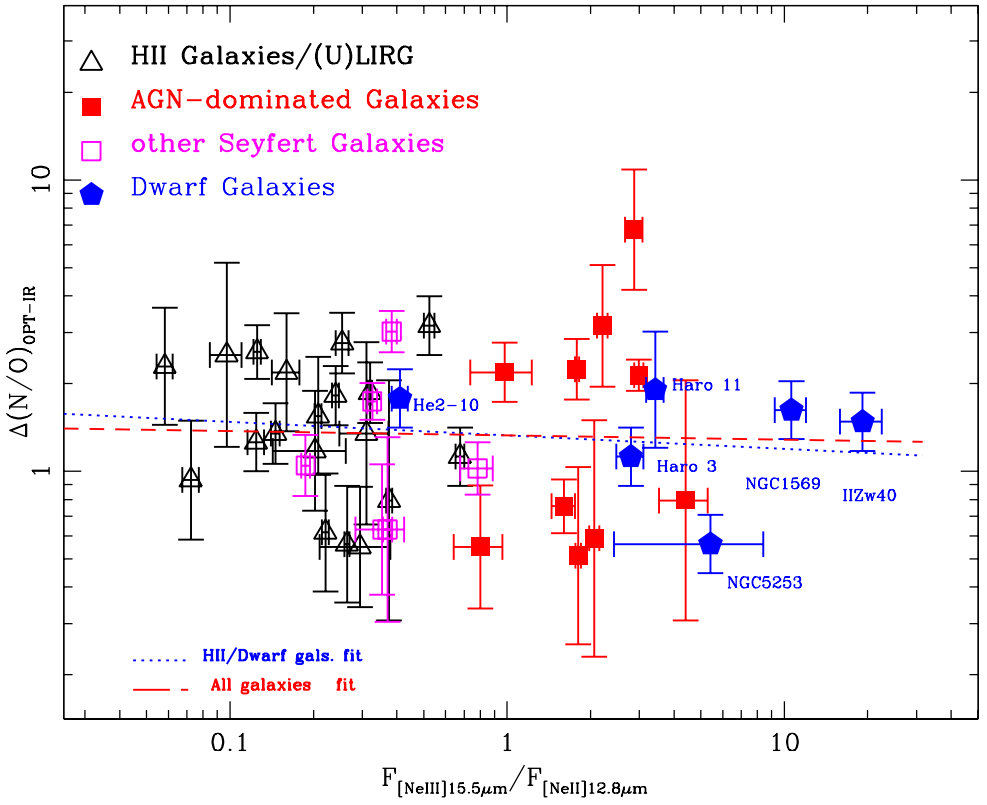

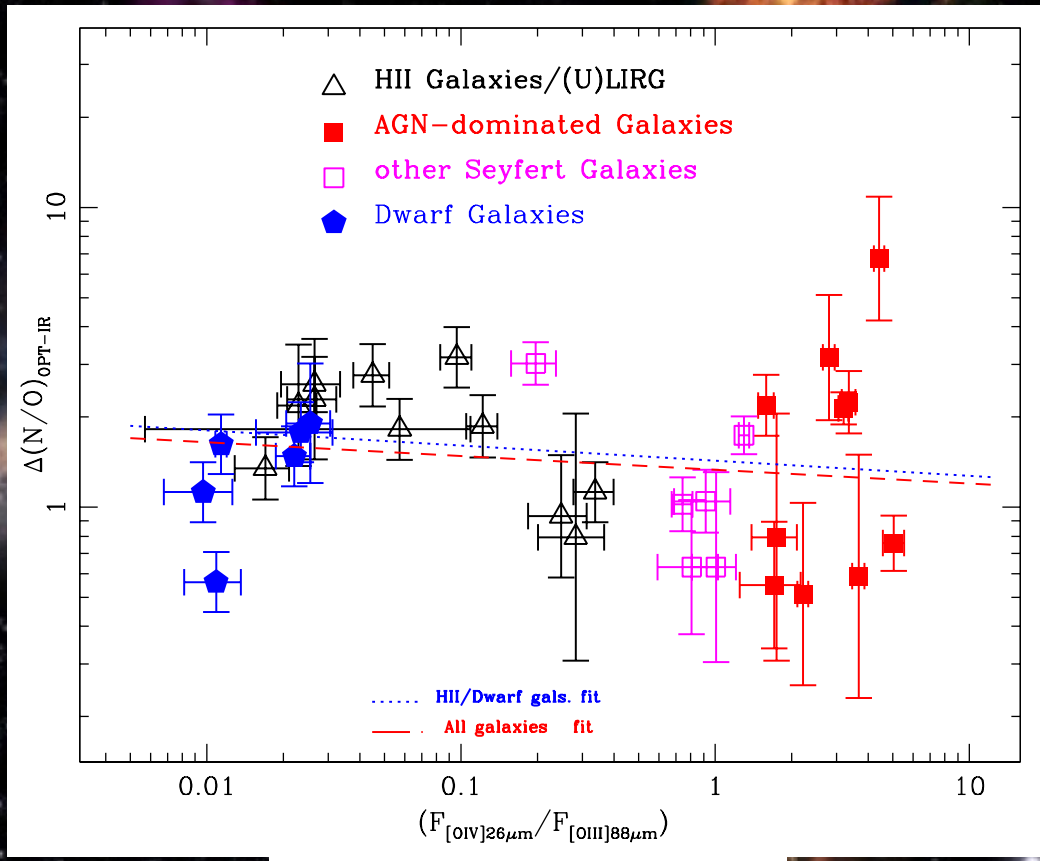

and [Oiv]/[Oiii]

decreasing trend but no correlation

Spinoglio et al. (2021), ApJ, in press & astro-ph: 2103.09253

Δ(N/O)≡(N/O)OPT-(N/O)IR search dependence of Δ(N/O) on density: [SII]λλ6716,6731A optical doublet

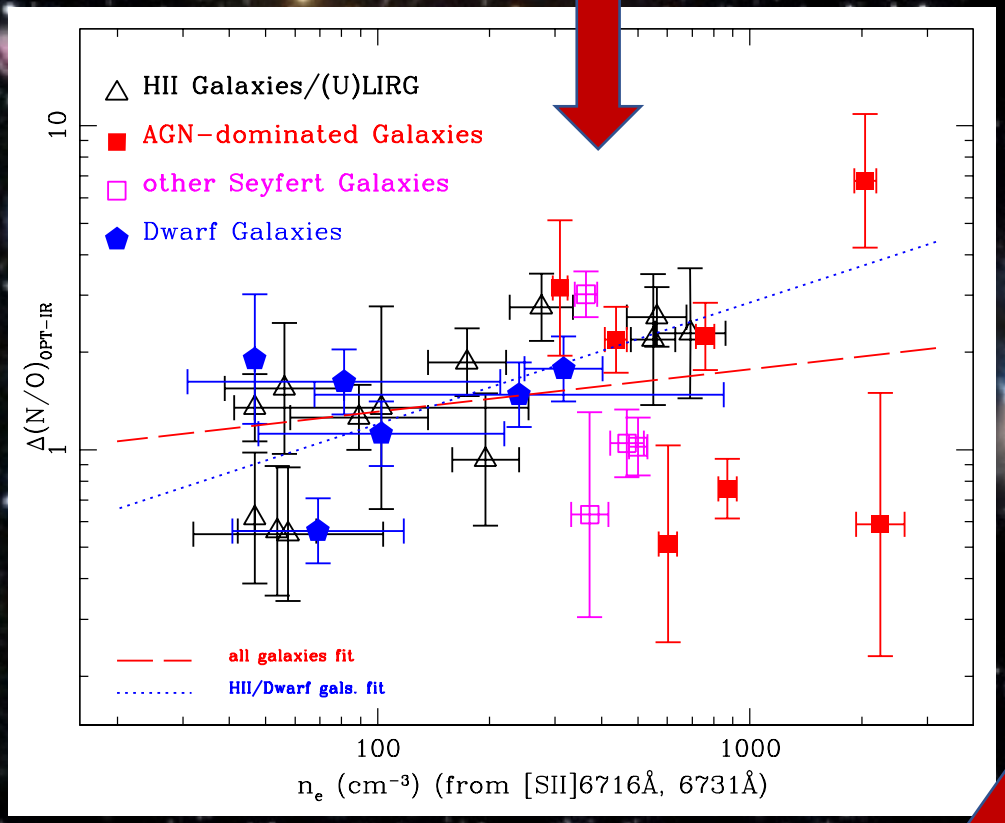

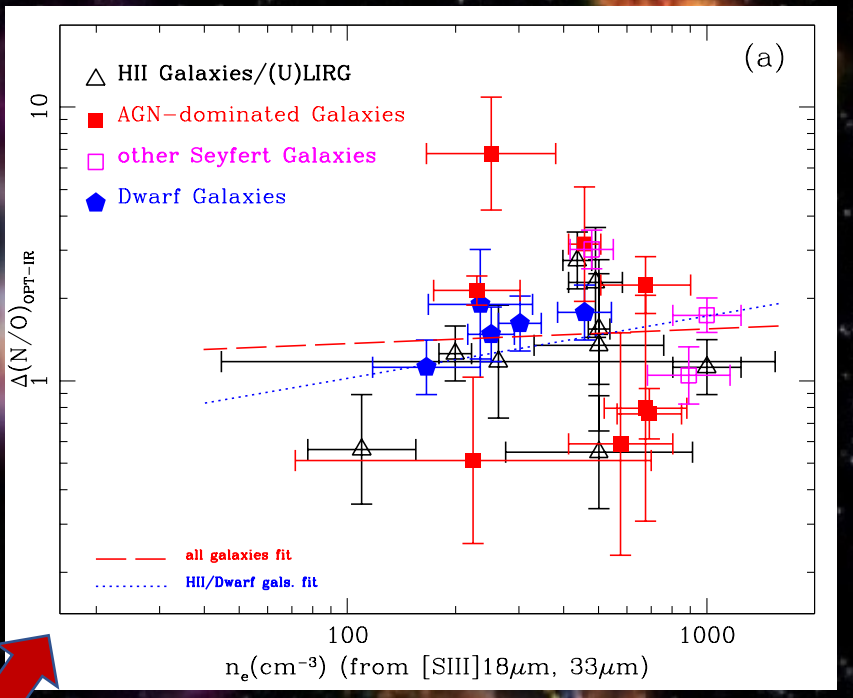

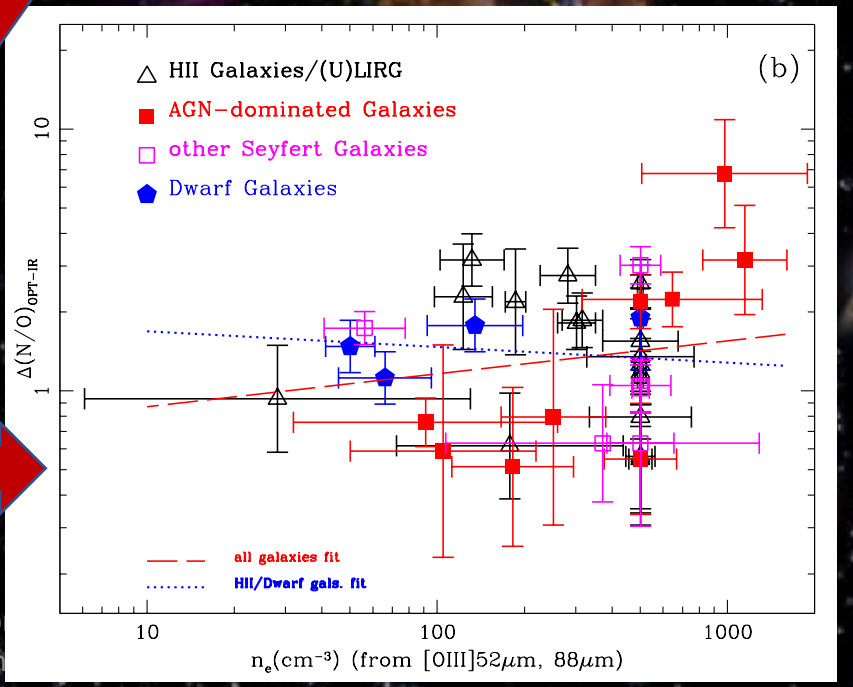

Δ(N/O)≡(N/O)OPT-(N/O)IR search dependence of Δ(N/O) on density: IR lines of [SIII]18,33μm and [OIII]52,88μm

Spinoglio et al. (2021), ApJ, in press & astro-ph: 2103.09253

Δ(N/O)≡(N/O)OPT-(N/O)IR search dependence of Δ(N/O) on extinction (from Balmer decrement)

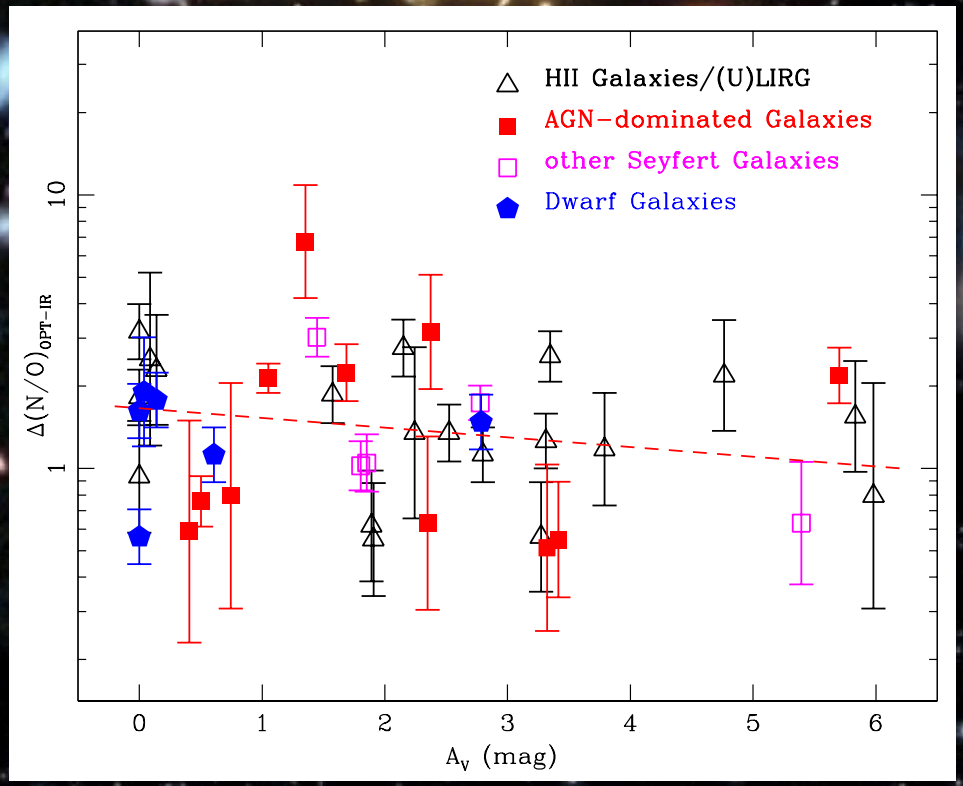

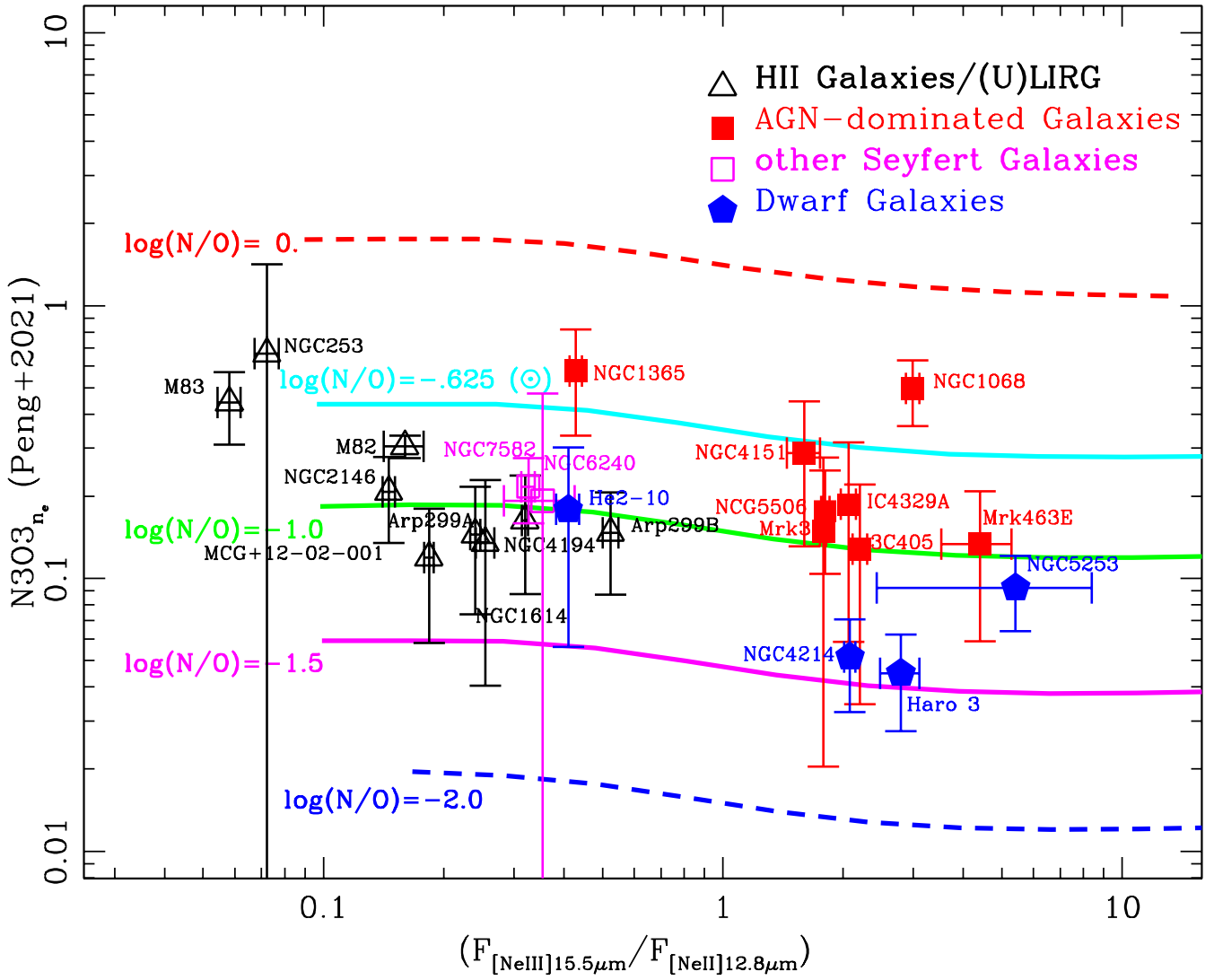

Following the work of Peng et al (2021), we have computed the density corrected $N3O3_{ne}$ ratio, according to their equation (4) which uses the [Oiii] FIR line fluxes to correct the N/O ratio for the density depencence.

We have re-made the same plot of Peng et al. Fig. 3, with the whole dataset that we discussed here.

We confirm the result of Peng et al., which confirms in an independent way our results.

A possible explanation (speculative)

Evolutionary effect?

- Koppen & Hensler 2005 scheme for N/O-OH track after accretion event.
- Optical emitting gas ➔ external layers
- IR ➔ lower N/O ratios due to the yields from young massive (emdebbed) stars producing more oxygen

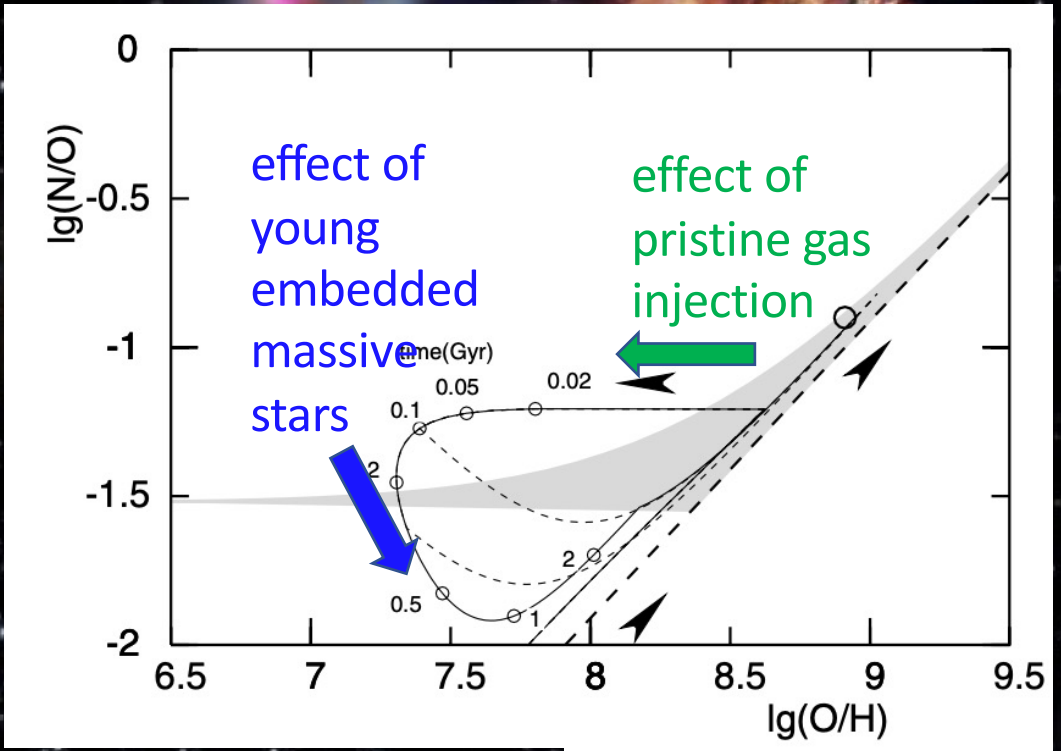

Köppen & Hensler 2005

conclusions

- N/O essential to constrain chemical evolution in galaxies (e.g. SFE, IMF, gas accretion, winds metal-loading factor)
- Far-IR N and O lines are excellent N/O tracers (see also Peng et al. 2021), observable at high-z with ALMA
- We analysed SOFIA/FIFI-LS + Herschel/PACS observations for 47 galaxies with [NIII]57µm and [OIII]52,88µm. Largest sample so far.
- N/O - O/H relation derived from IR tracers. Trends consistent with optical but N/O_IR ~ 0.3 dex lower for galaxies with the highest N/O_opt
- Discrepancy not explained by ionization structure, DIG contamination, or extinction ([OII]3727AA absorption)
- Evolutionary effect? Koppen & Hensler 2005 scheme for N/O-O/H track after accretion event. Optical emitting gas -> external layers, IR -> lower N/O ratios due to the yields from young massive (emdebbed) stars.
- The optical-to-IR abundance discrepancy analyzed in this work warns on the use of optical tracers to study the N/O abundances in galaxies at high redshift, e.g. using future James Webb Space Telescope observations of their rest-frame optical spectrum. ALMA observations in the FIR might be necessary.
- SOFIA in the nearby universe can map N and O FIR lines in the disk of resolved galaxies to understand which are the regions where the difference with the optical is larger (arms, inter-arms, center, etc.).
- ➔ need more observations of [OIII]52 & [NIII]57 lines (missed by Herschel) ... also in southern hemisphere
- ➔ important to improve the SOFIA FIFI-LS sensitivity: unique instrument to do this science